

SUPPLEMENTARY INFORMATION

Manuscript: “Pericentrosomal targeting of Rab6 secretory vesicles by Bicaudal-D related protein-1 (BICDR-1) regulates neuritogenesis” by Schlager et al.

SUPPLEMENTAL FIGURE LEGENDS

Figure S1. BICDR proteins are similar to BICD and conserved across species

(A, B) Phylogenetic tree of BICDR-1 and BICDR-2 homologues.

(C) Sequence alignment of mouse BICD1, BICD2, BICDR-1 and BICDR-2 (black: identical in all four sequences, dark gray: identical in three out of four sequences, light gray: identical in two out of four sequences).

Figure S2. BICDR-1 binds to Rab6 and accumulates around the centrosome

(A) Yeast two hybrid analysis. RAB6A-Q72R, Rab6A-T27N and Rab6A-WT were linked to LexA and BICDR-1 (1-577), BICDR-1 (382-577), BICD2 (586-820) and BICD2 (336-820) were fused to a GAL4 activation domain. Interaction strength was scored according to the time needed for β -galactosidase reporter to generate visible blue-colored yeast colonies on X-Gal containing filters in a colony filter lift assay: +++ 0-30 min, ++ 30-60 min, + 60-180 min and - no β -galactosidase activity.

(B) GST-pull down assay with GST or GST-Rab6A and extracts of Hek293T cells expressing GFP-BICD2-C. GST-Rab6A pull down assays were performed in the presence of an increasing amount of purified His-BICDR-1C. GFP-BICD2-C and His-BICDR-1C were detected by Western blotting with antibodies against GFP and His respectively.

(C-E) Representative images of endogenous BICDR-1 in Vero cells stained using antibodies #12 and #13.

(F) Boxed area indicated in C stained for BICDR-1 (green) and Rab6A (red).

(G) Vero cell stained for BICDR-1 (red) and α -tubulin (green).

(H) Vero cell stained for BICDR-1 (green) and F-actin, by phalloidin-A564 (red).

(C-H) Solid lines indicate the cell edge and dashed lines indicate the nucleus, Scale bars: C, E, G, H 10 μ m, D 50 μ m.

Figure S3. Pericentrosomal BICDR-1 localization depends on the microtubule cytoskeleton

(A) Vero cell treated with either Nocodazole (10 μ M for 30 minutes, left) or Cytochalasin-D (10 μ M for 30 minutes, right), fixed and stained for BICDR-1.

(B) Western blot analysis of Vero cell extracts cultured for 3 days after transfection with Rab6A specific siRNAs.

(C) Vero cells transfected with γ -tubulin shRNA (top, *) or untransfected (bottom) and stained for α -tubulin (red) and BICDR-1 (green).

(D) Vero cells transfected with Rab6A specific siRNA (right) and untransfected (left). Stained for BICDR-1 (green) and Rab6A (red).

(C-D) Solid lines indicate the cell edge and dashed lines indicate the nucleus. Inserts show magnifications of boxed areas. Scale bars, 10 μ m.

Figure S4. Characterization of BICDR-1 siRNAs

(A) Western blot analysis of Vero cell extracts cultured for 3 days after transfection with the indicated siRNAs.

(B) Percentage of cells expressing pericentrosomal BICDR-1 4 days after transfection with indicated siRNAs (average \pm SEM; control, n=3040; oligo88, n=876; oligo89, n=349; oligo90, n=359 cells).

(C) Representative image of Vero cells 4 days after transfection with BICDR-1-Oligo 88 siRNA and stained for BICDR-1 (green) and DAPI (blue).

(D) Vero cell transfected with BICDR-1 specific siRNAs, fixed and stained for endogenous BICDR-1 (green), Rab6A (red) and α -tubulin (blue). Solid lines indicate the cell edge and dashed lines indicate the nucleus. Inserts show magnifications of boxed areas.

(E) Quantification of pericentrosomal Rab6A staining intensity in control cells and cells transfected with BICDR-1 specific siRNAs (control, n=7; BICDR-1 siRNA, n=6 cells).

(F) MT nucleation rate in Vero cells transfected with either EB3-GFP (control; n=10 cells) or EB3-GFP and BICDR-1 shRNA (n=10 cells). MT growth velocity in Vero cells transfected with either mCherry-tubulin (control; n=65 in 4 cells) or mCherry-tubulin and BICDR-1 shRNA (n=97 in 4 cells). MT shrinkage velocity in Vero cells transfected with either mCherry-tubulin (control; n=58 in 4 cells) or mCherry-tubulin and BICDR-1 shRNA (n=54 in 4 cells).

Scale bars: C 50 μ m; D 10 μ m.

Figure S5. BICDR-1 interacts with the dynein/dynactin motor complex

(A) Vero cell transfected with BICDR-1 specific siRNAs, fixed and stained for endogenous BICDR-1 (green) and p150^{glued} (red).

(B) Representative image of a Vero cell stained for endogenous BICDR-1 (green) and for IC74 (red).

(C) Representative image of HeLa cells with and without GFP-BICDR-1 (green) overexpression stained for IC74 (red).

Solid lines indicate the cell edge and dashed lines indicate the nucleus. Inserts show magnifications of boxed areas. Scale bars, 10 μm .

Figure S6. BICDR-1 organizes secretory vesicle distribution

(A) Vero cell transfected with mCherry-BICDR-1 (red) and NPY-GFP (green) fixed and stained for Rab6A (blue).

(B) HeLa cell transfected with GFP-BICDR-1 (green) and NPY-mRFP (red) fixed and stained for Rab6A (blue).

(C) TIRFM images of HeLa cells stably expressing NPY-Venus: untransfected (control) or transfected with mCherry-BICDR-1 (+BICDR-1). Inserts are time lapse images of boxed areas, with the cell center (*C*) to the left and the periphery (*P*) to the right. Arrows indicate vesicles that undergo exocytosis, arrowheads indicate control vesicles (to show that focus is maintained throughout the images). Time is indicated in seconds.

(D) Distribution of exocytotic events (red dots) during 400 seconds in a control and BICDR-1 overexpressing cell.

(E) Number (+/- SEM) of NPY-Venus vesicles (per 100 μm^2 cell surface area) in the cell periphery and center in control and BICDR-1 overexpressing cells (peripheral control n=633 vesicles, 1647 μm^2 ; peripheral+BICDR-1 n=136 vesicles, 1442 μm^2 ; central control n=358 vesicles, 1228 μm^2 ; central+BICDR-1 n=584 vesicles, 1250 μm^2 ; all measured in 8 cells during 400 seconds).

(F) Number (+/- SEM) of exocytotic events (per minute, 100 μm^2 cell surface area and 100 observed vesicles) in the cell periphery and center in control and BICDR-1 overexpressing cells (peripheral control n=35 events, 1647 μm^2 ; peripheral+BICDR-1 n=0 events, 1442 μm^2 ;

central control n=2 events, 1228 μm^2 ; central+BICDR-1 n=61 events, 1250 μm^2 ; all measured in 8 cells during 400 seconds).

(A-B) Solid lines indicate the cell edge and dashed lines indicate the nucleus. Inserts show magnifications of boxed areas. Scale bars, 10 μm . (C-D) Solid lines indicate the cell edge.

Figure S7. BICDR-1 recruits dynein/dynactin, Rab6A/B and secreted proteins to the neuronal cell body

(A-E) Hippocampal neurons transfected with GFP-BICDR-1 (green) at DIV0.25, fixed after 2 days and stained for IC74, p150^{glued}, Rab6A, Rab6B, EEA1 (red) and α -tubulin (blue).

(F-G) Hippocampal neuron transfected with mCherry-BICDR-1 (red), BDNF-GFP or GFP-Semaphorin3A (green) and β -Gal (blue) at DIV1, fixed after 2 days.

Inserts are magnifications of boxed areas. Scale bar, 10 μm .

Fig. S8. Characterization of Rab6A/B antibodies and shRNAs in neurons

(A) Western blots of HeLa cell lysates containing GFP-Rab6A or GFP-Rab6B probed with indicated antibodies.

(B) Hippocampal neuron fixed at DIV3 and stained for Rab6A (red) and Rab6B (green). Inserts show magnifications of boxed area in a different focal plane, $r_p=0.8$.

(C-E) Hippocampal neurons (DIV3) stained for Rab6A (green), Rab6B (blue). Neurons indicated with an asterisk were transfected at DIV0.25 with indicated shRNAs and an mRFP or β -galactosidase fill (red).

(C) Inserts show magnifications of boxed areas. Scale bar, 10 μm .

Fig. S9. Model: BICDR-1 regulates Rab6 vesicle transport in developing neurons

Schematic model showing trafficking of Rab6 secretory vesicles (red) during neuronal development. In young neurons all microtubule minus ends face inward, recruitment of dynein motors to Rab6 vesicles by BICDR-1 will cause them to accumulate around the centrosome in the cell body. Under normal circumstances levels of BICDR-1 (green) rapidly decline, allowing anterograde transport of Rab6 vesicles from the cell body into the growing neurites. Under experimental conditions, with persistent levels of BICDR-1, Rab6 vesicles lose their anterograde transport ability, secretory vesicles remain in the cell body and neurite outgrowth is impaired.

SUPPLEMENTAL MOVIE LEGENDS

Movie S1:

GFP-Rab6A (left), mCherry-BICDR-1 (middle) and merge (right) in hippocampal neurons (DIV2) visualized using TIRFM. This video corresponds to Figure 5D. Total time 20 seconds. Acquired at 10 frames per second. 3x sped up.

Movie S2:

MRC5 cell transfected with NPY-Venus, visualized using TIRFM. Total time 150 seconds. Acquired at 2 frames per second. 15x sped up.

Movie S3:

Detail of a HeLa cell stably expressing NPY-Venus, visualized using TIRFM. This video corresponds to Figure S6B (control). Total time 3.6 seconds. Acquired at 10 frames per second. Not sped up.

Movie S4:

Detail of a HeLa cell stably expressing NPY-Venus and transfected with mCherry-BICDR-1, visualized using TIRFM. This video corresponds to Figure S6B (+BICDR-1). Total time 3.6 seconds. Acquired at 10 frames per second. Not sped up.

SUPPLEMENTAL MATERIALS AND METHODS

Antibodies and reagents

The following primary and secondary antibodies were used in this study: mouse monoclonal antibodies against Rab6A/Rab6A' (Matanis et al, 2002); human-anti-EEA1 (gift from M.J. Fritzler, University of Calgary (Selak et al, 2000)); rabbit anti- BICD2 (Hoogenraad et al, 2001); mouse anti-galactosyl transferase (gift from E.G. Berger, University of Zürich (Berger et al, 1981)). The following antibodies were obtained from commercial sources: rabbit anti-GFP, rat anti- α -tubulin (Abcam), mouse anti-actin, mouse anti-dynein IC74, mouse anti-Tau (Chemicon), mouse anti-p150^{glued}, mouse anti-GM130, mouse anti- γ -adaptin, mouse anti-EEA1 (BD Biosciences), rabbit anti-dynein heavy chain, rabbit anti-HA (Santa Cruz), sheep anti-TGN46 (Serotec), mouse anti-Tuj1 (Covance), HRP conjugated anti-Flag, mouse anti-MAP2, mouse anti- α -tubulin, mouse anti- γ -tubulin (Sigma), rabbit anti- β -galactosidase (MP Biomedicals), mouse anti-His (Qiagen), rabbit anti-Kif1C (Cytoskeleton) and mouse anti- β -galactosidase (Promega). We also used phalloidin-Alexa594, Alexa350-, Alexa488-, Alexa568- (Invitrogen), Cy3-, FITC- (Jackson) and HRP-conjugated secondary antibodies (Dako).

Antibody generation

cDNAs encoding BICDR-1 amino acids 1–146 and 161-387 were cloned into pGEX-4T (GE Healthcare) to create glutathione-*S*-transferase (GST) fusion proteins, and into pET-32A (Novagen) to create His-tagged fusion proteins. GST-BICDR-1 fusion proteins were induced in BL21 *Escherichia coli* cells by isopropyl β -D-1-thiogalactopyranoside and purified using glutathione-Sepharose 4B beads (GE Healthcare) according to the manufacturer's instructions. Purified proteins were concentrated using Centricon (Millipore) and injected into New Zealand White Rabbits in a suspension of Ribi adjuvant (Sigma). Sera #12 and #13 are against BICDR-1 amino acids 1–146 and 161-387 respectively. His-BICDR1 fusion proteins were induced in Rosetta bacteria, and purified using Nickel beads (Qiagen) according to the manufacturer's protocol. His-tagged fusion proteins were coupled to cyanogen bromide-activated Sepharose 4B-columns (GE Healthcare) and used to purify BICDR-1 antibodies. Both #12 and #13 were used at 1:50 dilution for immunofluorescence (IF) and 1:500 for western blot (WB). Rat monoclonal antibodies against Rab6B were generated using GST fusions of Rab6B by Absea (Beijing, China) and used 1:10 for IF and 1:250 for WB.

Expression Constructs and siRNA

The following mammalian expression plasmids have been described: p β actin-HA- β -galactosidase (Hoogenraad et al, 2005), pSuper vector (Brummelkamp et al, 2002). BICDR-1, BICD2, Rab6A, Rab6B, p50, p150^{glued}, NPY, Semaphorin3A and BDNF constructs were prepared by a PCR-based strategy using the following cDNAs: BICDR-1 (IMAGE clone 5361390), BICD2 (Hoogenraad et al, 2001), Rab6A (Matanis et al, 2002), Rab6B (Opdam et al, 2000), p50, p150^{glued} (Hoogenraad et al, 2003), NPY (Nagai et al, 2002), Semaphorin3A (De Wit et al, 2005) and BDNF (Jaworski et al, 2005). Subsequently PCR products were subcloned in pGW1-, pGW2- and p β actin-expression vectors (Hoogenraad et al, 2005). The following shRNA sequences were used in this study: The Rab6A (CACCTATCAGGCAACAATT) and the Rab6B (CACCTACCAGGCAACCATC) sequences targeting rat Rab6A mRNA (NM_053366) and Rab6B mRNA (NM_001108775) were designed based on a previously published sequence (Young et al, 2005). The γ -Tubulin (GGAGGACATGTTCAAGGAC) sequence targeting human γ -Tubulin-1 and γ -Tubulin-2 mRNA sequences (NM_001070.4 and NM_016437.2 respectively) was based on a previously published sequence (Alvarado-Kristensson et al, 2009). The Kif1C (CCCTTGATGTCTGAATGCCTT) sequence targeting rat Kif1C mRNA (NM_145877.1) was designed by using the siRNA selection program at the Whitehead Institute for Biomedical Research (<http://jura.wi.mit.edu/bioc/siRNAext/home.php>) (Yuan et al, 2004). The complementary oligonucleotides were annealed and inserted into a pSuper vector (Brummelkamp et al, 2002). The BICDR-1 (CCAAAGGCTATTGGATCAG) sequence targeting human BICDR-1 (NM_207311) was based on Ambion siRNA 149590. The complementary oligonucleotides were annealed and inserted into a modified pSuper vector, designed to co-express either mRFP or GFP in addition to the shRNA (Johansson et al, 2007). We used the following siRNAs: DHC#1 5'-CGUACUCCCGUGAUUGAUG-3' (siRNA 118309, Ambion); DHC#2 CGUACUCCCGUGAUUGAUG (siRNA 118309, Ambion); BICDR-1-Oligo88 5'- GCACUUAGAGCAAGAGAAA-3' (siRNA 149588, Ambion); BICDR-1-Oligo89 5'- GCAGAUCGAGAAAAAUCAC-3' (siRNA 149589, Ambion); BICDR-1-Oligo90 5'- CCAAAGGCUAUUGGAUCAG-3' (siRNA 149590, Ambion); p150#1 5'-GUAUUUGAAGAUGGAGCAG-3'; Rab6#1 5'-GACAUCUUUGAUCACCAGA-3' (Young et al, 2005); Rab6#2 5'-CACCUAUCAGGCAACAAUU-3' (Young et al, 2005).

Primary Sequence analysis

A BLASTP search was performed using mouse BICD1 (NP_033883) and mouse BICD2 (NP_084067.1) sequences to identify mouse BICDR-1 (NP_001074277.1) a further BLASTP search using BICDR-1 sequence identified mouse BICDR-2 (NP_722479.1). Sequences were aligned using the t-coffee program (Poirot et al, 2003) and primary structure was analyzed using Coils: (http://www.ch.embnet.org/software/COILS_form.html). BICDR-1 and BICDR-2 orthologues were identified using Homologene (<http://www.ncbi.nlm.nih.gov/homologene>) and Ensembl (www.ensembl.org), aligned with ClustalW (<http://www.ch.embnet.org/software/ClustalW.html>) and phylogenetic trees were made using Treeview X (<http://darwin.zoology.gla.ac.uk/~rpage/treeviewx>).

Hippocampal neuron cultures

Primary hippocampal cultures were prepared from embryonic day 18 (E18) rat brains (Banker, 1998). Cells were plated on coverslips coated with poly-L- lysine (30 µg/ml) and laminin (2 µg/ml) at a density of 75,000/well. Hippocampal cultures were grown in Neurobasal medium (NB) supplemented with B27, 0.5 mM glutamine, 12.5 µM glutamate and penicillin/streptomycin as described in Jaworski et al. (Jaworski et al, 2009).

Transfection and immunohistochemistry of neuronal cultures

Hippocampal neurons were transfected using Lipofectamine 2000 (Invitrogen). Briefly, DNA (3.6 µg /well) was mixed with 3 µl Lipofectamine 2000 in 200 µl NB, incubated for 30 minutes and then added to the neurons in NB at 37°C in 5% CO₂ for 45 min. Next, neurons were washed with NB and transferred in the original medium at 37°C in 5% CO₂ for 1-4 days. For transfection at DIV0 the procedure was modified by plating neurons in DMEM/Ham'sF10 (50/50%) medium containing 10% FCS and 1% penicillin/streptomycin, after 3 hours the medium was replaced with supplemented NB medium. At 6 hours after plating DNA/Lipofectamine 2000/NB was added to the neurons followed by 90 minute incubation at 37°C and 5% CO₂. 7.5 hours after plating neurons were washed in NB and returned to the original supplemented NB medium at 37°C and 5% CO₂ for 1-4 days. For immunocytochemistry, neurons were fixed for 10 minutes with 4% paraformaldehyde/4% sucrose in phosphate-buffered saline (PBS) at room temperature. After fixation cells were washed three times in PBS for 10 min at room temperature, and incubated with primary antibodies in GDB buffer (0.2% BSA, 0.8 M NaCl, 0.5% Triton X-100, 30 mM phosphate buffer, pH 7.4) overnight at 4°C. Neurons were then washed three times in PBS for 30 min at

room temperature and incubated with Alexa-conjugated secondary antibodies in GDB for 1-2 hr at room temperature and washed three times in PBS for 30 min. Slides were mounted using Vectashield mounting medium (Vector laboratories).

Hela and Vero cell culture and siRNA transfection

Hela and Vero cells were cultured in DMEM/Ham's F10 (50/50%) medium containing 10% FCS and 1% penicillin/streptomycin. Four to five days before fixation cells were plated at a dilution of ~1:80, and allowed to attach overnight. Cells were transfected with siRNAs at a final concentration of 5-20 nM, using Hiperfect (Qiagen) according to the manufacturers guidelines. A second transfection with the same siRNA concentration was performed one or two days later. Three or four days after the initial transfection, lysates were prepared and analyzed on immunoblot or cells were fixed and analyzed by immunofluorescence.

Transfection and immunofluorescence of cultured Hela, Vero and MRC5 cells

Hela, Vero and MRC5 cells were cultured in DMEM/Ham's F10 (50/50%) medium containing 10% FCS and 1% penicillin/streptomycin. One day before transfection, cells were plated at 1:20 in Lab-tek chamber slides (Nunc) or on glass coverslips. Cells were transfected with Superfect transfection reagent (Qiagen) or Fugene6 (Roche) according to the manufacturers protocol and incubated overnight. Stable Hela clones were selected with fluorescence activated cell sorting (FACS) and cultured in the presence of 0.4 mg/ml G418 (Roche).

Cells were fixed in 4% paraformaldehyde for 10 min at room temperature followed by 5 min in 0.1% Triton X-100 in PBS. Slides were blocked in 0.5% BSA/0.02% glycine in PBS and labeled with primary antibody either for 2 h at room temperature or overnight at 4°C. Slides were washed three times with 0.05% Tween20 in PBS, labeled with secondary antibodies for 1 hour at room temperature, washed three times with 0.05% Tween20 in PBS and mounted using Vectashield mounting medium (Vector laboratories) (Hoogenraad et al, 2000).

Preparation of tissue extracts

For tissue Western blots, brain, spinal cord, kidney, lung, spleen, testis, ovary were dissected from P30 mice and placed in ice-cold PBS, pH7.4. For developmental Western blots, E10.5 (whole embryo), E13.5, E16, E18 and P1 (head only) mice were placed in ice-cold PBS, pH 7.4. Samples were homogenized in homogenization buffer (150 mM NaCl, 50 mM Tris, 0.1% v/v SDS, 0.5% v/v NP-40, pH8, 1x complete protease inhibitors; Roche), briefly sonicated,

centrifuged at 900 rcf, resuspended in SDS sample buffer and boiled for 5 minutes. Protein concentrations were measured using a BCA protein assay kit (Pierce) and 20 µg of protein was loaded in each lane for a subsequent Western blot analysis. DIV1, DIV3, DIV5 and DIV26 hippocampal neurons were directly lysed in 2x SDS sample buffer, briefly sonicated, boiled and subjected to immunoblotting.

GST-Rab pull down assays

GST-Rabs were expressed in *Escherichia coli* JM109 and purified using standard protocols as described previously (Itoh et al, 2008). Gluthathione-Sepharose 4B beads (GE Healthcare) coupled to each GST-Rab (Rab1-43) were incubated with COS7 cell lysates containing Flag tagged BICDR-1, BICDR-1-K512M, BICD2 or BICD2-K785M in the presence of 0.5 mM of guanosine 5'-O-(3-thio)triphosphate (GTP γ S). Bound BICDR-1 or BICD2 was detected by immunoblotting using HRP conjugated Flag antibody (Sigma). GST-Rabs were then stained with amido black to ensure that equivalent amounts of GST fusion proteins had been loaded.

For direct binding assays, 5 µg GST, GST-Rab6A or GST-Rab6B was immobilized on 25 µl glutathione Sepharose 4B beads and washed three times with buffer NE100 (20 mM HEPES, pH 7.5, 100 mM NaCl, 10 mM EDTA, 0.1% v/v Triton X-100), two times with buffer NL100 (20 mM HEPES, pH 7.5, 100 mM NaCl, 5 mM MgCl₂, 0.1% v/v Triton X-100) and finally two times with 500 µl buffer NL100 GTP γ S (20 mM HEPES, pH 7.5, 100 mM NaCl, 5 mM MgCl₂, 0.1% v/v Triton X-100, 50 µM GTP γ S) as described by Fuchs et al. (Fuchs et al, 2005). For the binding reaction, loaded beads were resuspended in 200 µl NL100 GTP γ S with approximately 4 µg His-BICDR-1-C or His-BICDR-1-C-K512M and incubated on a roller for 2 h at 4°C. After incubation, beads were pelleted by centrifugation and unbound protein was removed by washing four times with 1 ml NL100 GTP γ S. Bound protein was eluted directly in 40 µl 1× SDS sample buffer, analyzed on 12% SDS-PAGE gel and visualized on Western blot using anti-His antibody (Qiagen).

Rab6A-binding competition experiments were performed essentially as described for the direct binding assays, but with 2 µl GFP-BICD2C containing Hek cell lysate and either 0, 0.1 or 1 µl purified His-BICDR-1C in the binding reaction. GFP-BICD2C and His-BICDR-1 were detected on the same blot using anti GFP or anti His antibodies respectively.

Immunoprecipitation

Hela cells were cultured in DMEM/Hams-F10 (50/50%) medium containing 10% FCS and 1% penicillin/streptomycin and were transfected using Lipofectamine2000 (Invitrogen). Cells

were harvested 24 h after transfection, by scraping the cells in ice-cold PBS and lysing cell pellets in lysis buffer (25 mM Tris-HCl, pH 8.0, 100 mM NaCl, 1.0% Triton X-100, and protease inhibitors; Roche). Supernatant and pellet fractions were separated by centrifugation at 13,200 rpm for 5 minutes. Supernatants were mixed with an equal amount of lysis buffer, protein-A-agarose beads (GE Healthcare), and 3 μ g of mouse anti-GFP (Roche). Samples were incubated 4 hours while rotating at 4°C, centrifuged at 2000 rpm and pellets were washed 5-7 times with wash buffer (25 mM Tris-HCl, pH 8.0, 100 mM NaCl, 0.1 % NP40). Samples were eluted in SDS sample buffer, equally loaded onto SDS-PAGE gels and subjected to western blotting on polyvinylidene difluoride membrane. Blots were blocked with 2% bovine serum albumin/0.05% Tween 20 in PBS and incubated with primary antibodies at 4°C overnight. Blots were washed with 0.05% Tween 20 in PBS three times for 10 min at room temperature and incubated with either anti-rabbit or anti-mouse IgG antibody conjugated to horseradish peroxidase (Dako). Blots were developed with enhanced chemiluminescent Western blotting substrate (Pierce).

Yeast two-hybrid analysis

Rab6A-Q72R, Rab6A-T27N, Rab6A wild type and Kif1C fragments were cloned into pBHA (lexA fusion vector) and tested against the indicated BICDR-1 and BICD2 fragments constructed in pGAD10 (GAL4 activation domain vector; Clontech). All constructs were generated by PCR-based strategy using the following cDNAs as templates: Rab6A (Matanis et al, 2002), Kif1C (KIAA clone 0706), BICDR-1 (IMAGE clone 5361390) and BICD2 (Hoogenraad et al, 2001). Yeast two-hybrid analysis was carried out using the L40 yeast strain harboring HIS3 and β -galactosidase as reporter genes as described previously (Niethammer & Sheng, 1998). β -galactosidase activity was detected using colony filter lift assays and scored according to time needed for β -galactosidase reporter to generate visible blue-colored yeast colonies on X-Gal-containing filters.

***In situ* hybridization**

BICDR-1-specific riboprobes were transcribed from PCR fragments encompassing nucleotides 1-1059 (probe #1 and #2, sense and antisense respectively) and 1144-1734 (probe #3 and #4, sense and antisense respectively) of the full-length cDNA (IMAGE clone 5361390) constructed in pBluescriptII-ks⁺ using the DIG Probe Synthesis Kit (Roche) according to the manufacturers protocol.

Whole mount in situ hybridization were performed as previously described (Henrique et al, 1995). Cryosections were prepared and in situ hybridized as described previously (Schaeren-Wiemers & Gerfin-Moser, 1993).

Northern blotting

Rat tissue northern blots were obtained from BD Biosciences (Rat MTN Blot, #7764-1), radiolabelled according to the manufacturers guidelines and visualized using a Typhoon imager (GE Healthcare).

Image acquisition and time-lapse live cell imaging

Images of fixed cells were collected with a Leica DMRBE microscope equipped with PLFluotar 40x 1.0 N.A. and PLFluotar 100x 1.3 N.A. oil objectives, FITC/EGFP filter 41012 (Chroma), Texas Red filter 41004 (Chroma), DAPI filter 31000 (Chroma) and an ORCA-ER-1394 CCD camera (Hamamatsu). Images were projected onto the 12-bit CCD chip at a magnification of 0.1 $\mu\text{m}/\text{pixel}$. To optimize images in Supplemental Fig. 8C-E an image generated by subtracting a low-pass filtered image from the original image was added to the original image.

Simultaneous dual color (green and red) time-lapse live cell imaging was performed on an inverted research microscope Nikon Eclipse TE2000E (Nikon) with a CFI Apo TIRF 100x 1.49 N.A. oil objective (Nikon), equipped with a Coolsnap and a QuantEM EMCCD cameras (Roper Scientific) controlled by MetaMorph 7.1 software (Molecular Devices). For excitation we used a HBO 103 W/2 Mercury Short Arc Lamp (Osram) and a Chroma EGFP/mCherry filter cube. To separate emissions we used DualView (Optical Insight) with emitters HQ530/30M and HQ630/50M (Chroma) and the beam splitter 565DCXR (Chroma). During imaging cells were maintained at 37°C in the standard culture medium in a closed chamber with 5% CO₂ (Tokai Hit; INUG2-ZILCS-H2). To depolarize neurons, KCl was added to the medium to a final concentration of 60 mM.

Image Analysis and Quantification

Quantification of fluorescent intensity: Ratios of pericentrosomal versus centrosomal intensities were determined by measuring the mean gray value of a 34 μm^2 area around the centrosome and in an area of equal size in the cytoplasm using ImageJ (<http://rsb.info.nih.gov/ij/index.html>). Ratios were averaged over multiple cells and experiments and a statistical analysis was performed with student's t test assuming a two-

tailed and unequal variation. Rab6A/B signal intensities in Fig. 6B were measured by determining the mean gray value of a $107 \mu\text{m}^2$ area in the cell body using ImageJ, the mean gray value of an adjacent $107 \mu\text{m}^2$ area without cells was subtracted as background. Intensities were averaged over multiple cells and a statistical analysis was performed with student's t test assuming a two-tailed and unequal variation. Pericentrosomal Rab6A intensities in Fig. S4E were measured by determining the location of the centrosome in the α -tubulin channel and subsequently measuring the average gray value in the corresponding region of the Rab6A channel using ImageJ. Intensities were normalized to area and averaged over multiple cells and a statistical analysis was performed with student's t test assuming a two-tailed and unequal variation. Control intensity was set at 1.

Analysis of colocalization: Pearson's coefficient (r_p) was determined using the JACoP plugin (Bolte & Cordelieres, 2006) for ImageJ.

Measurement of neurite outgrowth: To measure neurite length we used β -gal, GFP or mRFP as an unbiased cell-fill. Hippocampal neurons were transfected with constructs indicated in Figure 8 at DIV0.25 as described earlier, empty pGW1-HA and pSuper vectors were used as controls. Neurons were cultured at 37°C and 5% CO_2 for 2, 3 or 4 days, at the appropriate time the neurons were fixed and subjected to immunofluorescent staining. MAP2 or Tau counterstaining was used to determine the dendrite and axon length respectively. Confocal images were acquired using a LSM510 confocal microscope (Zeiss) with a dry 20x objective, neurites were measured from cell body to tip using MetaMorph (Universal Imaging Corporation) software. Data were averaged over multiple cells and experiments and a statistical analysis was performed with student's t test assuming a two-tailed and unequal variation.

Measurement of exocytotic vesicles and events: Data were normalized to area (exocytotic vesicles) or to time, area and number of observed vesicles (exocytotic events). Subsequently data were averaged over multiple cells and a statistical analysis was performed with a non parametrical Mann-Whitney U-test.

Microtubule dynamics: Microtubule growth and shrinkage rates were measured using EB3-GFP and mCherry-tubulin respectively. Microtubule nucleation was measured within a circular region of $3 \mu\text{m}$ in diameter using EB3-GFP. Subsequently data were averaged over multiple cells and a statistical analysis was performed with a non parametrical Mann-Whitney U-test.

Measurement of vesicle distribution: To determine the number of NPY-GFP, BDNF-GFP or GFP-Semaphorin3A positive vesicles in neurites, GFP positive vesicles were counted by hand and subsequently the corresponding neurite length was measured in the β -Gal channel using ImageJ. Data were normalized to length and averaged over multiple cells, a statistical analysis was performed with student's t test assuming a two-tailed and unequal variation.

In the figures the results of statistical analyses are indicated as follows: ns – no statistically significant difference; * - statistically significant with $p < 0.05$; ** -statistically significant with $p < 0.01$; *** - statistically significant with $p < 0.001$.

Zebrafish maintenance and breeding

Fish were raised and kept under standard laboratory conditions at 28.5°C (Ekker et al, 1992). Embryos were staged and fixed at specific hours or days post fertilization (hpf or dpf) as described by Kimmel et al. (Kimmel et al, 1995). To better visualize internal structures in some experiments embryos were incubated with 0.2mM 1-phenyl-2-thiourea (Sigma) to inhibit pigment formation (Ekker et al, 1992).

Isolation of zebrafish BICDR-1 orthologue

A TBLASTX search was performed on the Zebrafish Genome Browser on the World Wide Web to identify the zebrafish BICDR-1 orthologue using mouse and human sequences. A single orthologue was identified (XM_689029). To clone the complete ORF of the zebrafish orthologue RT-PCR primers were designed to amplify the complete open reading frame based on the predicted sequences. The ORF was isolated by RT-PCR from 48hpf embryos subcloned and sequenced.

Zebrafish whole-mount in situ hybridization

Embryos were collected and processed for whole-mount in situ hybridization as previously described (Thisse et al, 1993). Digoxigenin-labeled riboprobe used in this study were synthesized from a template linearized and transcribed. Digoxigenin-labeled probes were visualized with NBT/BCIP coloration reactions.

Zebrafish embryonic microinjections

Two BICDR-1 morpholinos were designed to target the translation start site of the gene (BICDR-1 TBMO) and to block the splicing of the transcript at the exon 3-intron 3 splice junction (BICDR-1 SBMO). The sequences were as follows:

BICDR-1 TBMO: 5' TATGGGTCCTCGCCAGCCATGATTC 3'

BICDR-1 SBMO: 5' AGCTCTTACCTGTTCTCATGATGT 3'

A mismatch control morpholino was generated for the BICDR-1 TBMO with the following sequence: BICDR-1 Mismatch Ctrl: 5' TATaGGTgCTCGCCAcCCATcATaC 3'

Approximately 4 nl of 7 µg/µl of each morpholino was injected into 1-to 2-cell embryos using a gas-driven microinjection apparatus (PV820 WPI) through a micropipette.

Zebrafish immunohistochemistry and vital dye staining

Embryos were processed for immunohistochemistry as previously described (Raible & Kruse, 2000). Proliferating cells were identified using a monoclonal anti-phosphohistone H3 antibody (Upstate) (Ajiro et al, 1996). Cells undergoing apoptosis were identified using an anti-activated Caspase-3 rabbit polyclonal antibody (BD Biosciences). Live embryos were stained for apoptotic cells with the vital dye Acridine Orange as previously described (Barrallo-Gimeno et al, 2004). The 300X stock solution (5 mg/ml in embryo media) was diluted to 1X concentration. Dechorionated embryos were then bathed in this solution for 20 minutes in the dark. Embryos were washed in fresh embryo media and analyzed under a fluorescent microscope.

REFERENCES

- Ajiro K, Yoda K, Utsumi K, Nishikawa Y (1996) Alteration of cell cycle-dependent histone phosphorylations by okadaic acid. Induction of mitosis-specific H3 phosphorylation and chromatin condensation in mammalian interphase cells. *J Biol Chem* **271**(22): 13197-13201
- Alvarado-Kristensson M, Rodriguez MJ, Silio V, Valpuesta JM, Carrera AC (2009) SADB phosphorylation of gamma-tubulin regulates centrosome duplication. *Nat Cell Biol* **11**(9): 1081-1092
- Banker G, Goslin, K. (1998) *Culturing Nerve Cells*, Second edn. Cambridge, MA: The MIT Press.
- Barrallo-Gimeno A, Holzschuh J, Driever W, Knapik EW (2004) Neural crest survival and differentiation in zebrafish depends on mont blanc/tfap2a gene function. *Development* **131**(7): 1463-1477
- Berger EG, Mandel T, Schilt U (1981) Immunohistochemical localization of galactosyltransferase in human fibroblasts and HeLa cells. *J Histochem Cytochem* **29**(3): 364-370
- Bolte S, Cordelieres FP (2006) A guided tour into subcellular colocalization analysis in light microscopy. *J Microsc* **224**(Pt 3): 213-232
- Brummelkamp TR, Bernards R, Agami R (2002) A system for stable expression of short interfering RNAs in mammalian cells. *Science* **296**(5567): 550-553
- De Wit J, De Winter F, Klooster J, Verhaagen J (2005) Semaphorin 3A displays a punctate distribution on the surface of neuronal cells and interacts with proteoglycans in the extracellular matrix. *Mol Cell Neurosci* **29**(1): 40-55
- Ekker M, Wegner J, Akimenko MA, Westerfield M (1992) Coordinate embryonic expression of three zebrafish engrailed genes. *Development* **116**(4): 1001-1010
- Fuchs E, Short B, Barr FA (2005) Assay and properties of rab6 interaction with dynein-dynactin complexes. *Methods Enzymol* **403**: 607-618
- Henrique D, Adam J, Myat A, Chitnis A, Lewis J, Ish-Horowicz D (1995) Expression of a Delta homologue in prospective neurons in the chick. *Nature* **375**(6534): 787-790
- Hoogenraad CC, Akhmanova A, Grosveld F, De Zeeuw CI, Galjart N (2000) Functional analysis of CLIP-115 and its binding to microtubules. *J Cell Sci* **113** (Pt 12): 2285-2297
- Hoogenraad CC, Akhmanova A, Howell SA, Dortland BR, De Zeeuw CI, Willemsen R, Visser P, Grosveld F, Galjart N (2001) Mammalian Golgi-associated Bicaudal-D2 functions in the dynein-dynactin pathway by interacting with these complexes. *EMBO J* **20**(15): 4041-4054
- Hoogenraad CC, Milstein AD, Ethell IM, Henkemeyer M, Sheng M (2005) GRIP1 controls dendrite morphogenesis by regulating EphB receptor trafficking. *Nat Neurosci* **8**(7): 906-915

- Hoogenraad CC, Wulf P, Schiefermeier N, Stepanova T, Galjart N, Small JV, Grosveld F, de Zeeuw CI, Akhmanova A (2003) Bicaudal D induces selective dynein-mediated microtubule minus end-directed transport. *EMBO J* **22**(22): 6004-6015
- Itoh T, Fujita N, Kanno E, Yamamoto A, Yoshimori T, Fukuda M (2008) Golgi-resident small GTPase Rab33B interacts with Atg16L and modulates autophagosome formation. *Mol Biol Cell* **19**(7): 2916-2925
- Jaworski J, Kapitein LC, Gouveia SM, Dortland BR, Wulf PS, Grigoriev I, Camera P, Spangler SA, Di Stefano P, Demmers J, Krugers H, Defilippi P, Akhmanova A, Hoogenraad CC (2009) Dynamic microtubules regulate dendritic spine morphology and synaptic plasticity. *Neuron* **61**(1): 85-100
- Jaworski J, Spangler S, Seeburg DP, Hoogenraad CC, Sheng M (2005) Control of dendritic arborization by the phosphoinositide-3'-kinase-Akt-mammalian target of rapamycin pathway. *J Neurosci* **25**(49): 11300-11312
- Johansson M, Rocha N, Zwart W, Jordens I, Janssen L, Kuijl C, Olkkonen VM, Neefjes J (2007) Activation of endosomal dynein motors by stepwise assembly of Rab7-RILP-p150Glued, ORP1L, and the receptor betalll spectrin. *J Cell Biol* **176**(4): 459-471
- Kimmel CB, Ballard WW, Kimmel SR, Ullmann B, Schilling TF (1995) Stages of embryonic development of the zebrafish. *Dev Dyn* **203**(3): 253-310
- Matanis T, Akhmanova A, Wulf P, Del Nery E, Weide T, Stepanova T, Galjart N, Grosveld F, Goud B, De Zeeuw CI, Barnekow A, Hoogenraad CC (2002) Bicaudal-D regulates COPI-independent Golgi-ER transport by recruiting the dynein-dynactin motor complex. *Nat Cell Biol* **4**(12): 986-992
- Nagai T, Ibata K, Park ES, Kubota M, Mikoshiba K, Miyawaki A (2002) A variant of yellow fluorescent protein with fast and efficient maturation for cell-biological applications. *Nat Biotechnol* **20**(1): 87-90
- Niethammer M, Sheng M (1998) Identification of ion channel-associated proteins using the yeast two-hybrid system. *Methods Enzymol* **293**: 104-122
- Opdam FJ, Echard A, Croes HJ, van den Hurk JA, van de Vorstenbosch RA, Ginsel LA, Goud B, Franssen JA (2000) The small GTPase Rab6B, a novel Rab6 subfamily member, is cell-type specifically expressed and localised to the Golgi apparatus. *J Cell Sci* **113** (Pt 15): 2725-2735
- Poirot O, O'Toole E, Notredame C (2003) Tcoffee@igs: A web server for computing, evaluating and combining multiple sequence alignments. *Nucleic Acids Res* **31**(13): 3503-3506
- Raible DW, Kruse GJ (2000) Organization of the lateral line system in embryonic zebrafish. *J Comp Neurol* **421**(2): 189-198

Schaeren-Wiemers N, Gerfin-Moser A (1993) A single protocol to detect transcripts of various types and expression levels in neural tissue and cultured cells: in situ hybridization using digoxigenin-labelled cRNA probes. *Histochemistry* **100**(6): 431-440

Selak S, Woodman RC, Fritzler MJ (2000) Autoantibodies to early endosome antigen (EEA1) produce a staining pattern resembling cytoplasmic anti-neutrophil cytoplasmic antibodies (C-ANCA). *Clin Exp Immunol* **122**(3): 493-498

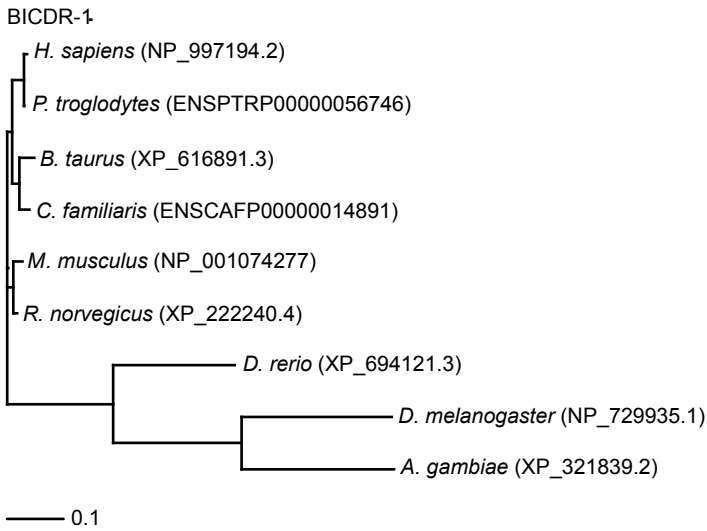
Thisse C, Thisse B, Schilling TF, Postlethwait JH (1993) Structure of the zebrafish snail gene and its expression in wild-type, spadetail and no tail mutant embryos. *Development* **119**(4): 1203-1215

Young J, Stauber T, del Nery E, Vernos I, Pepperkok R, Nilsson T (2005) Regulation of microtubule-dependent recycling at the trans-Golgi network by Rab6A and Rab6A'. *Mol Biol Cell* **16**(1): 162-177

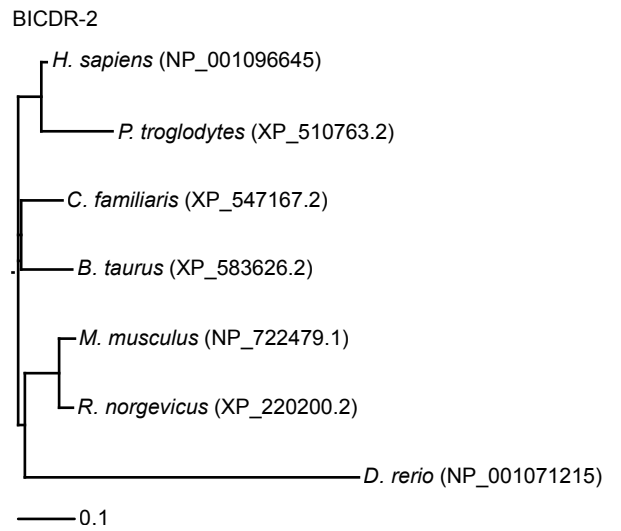
Yuan B, Latek R, Hossbach M, Tuschl T, Lewitter F (2004) siRNA Selection Server: an automated siRNA oligonucleotide prediction server. *Nucleic Acids Res* **32**(Web Server issue): W130-134

Schlager et al., Supplemental Figure 1

A



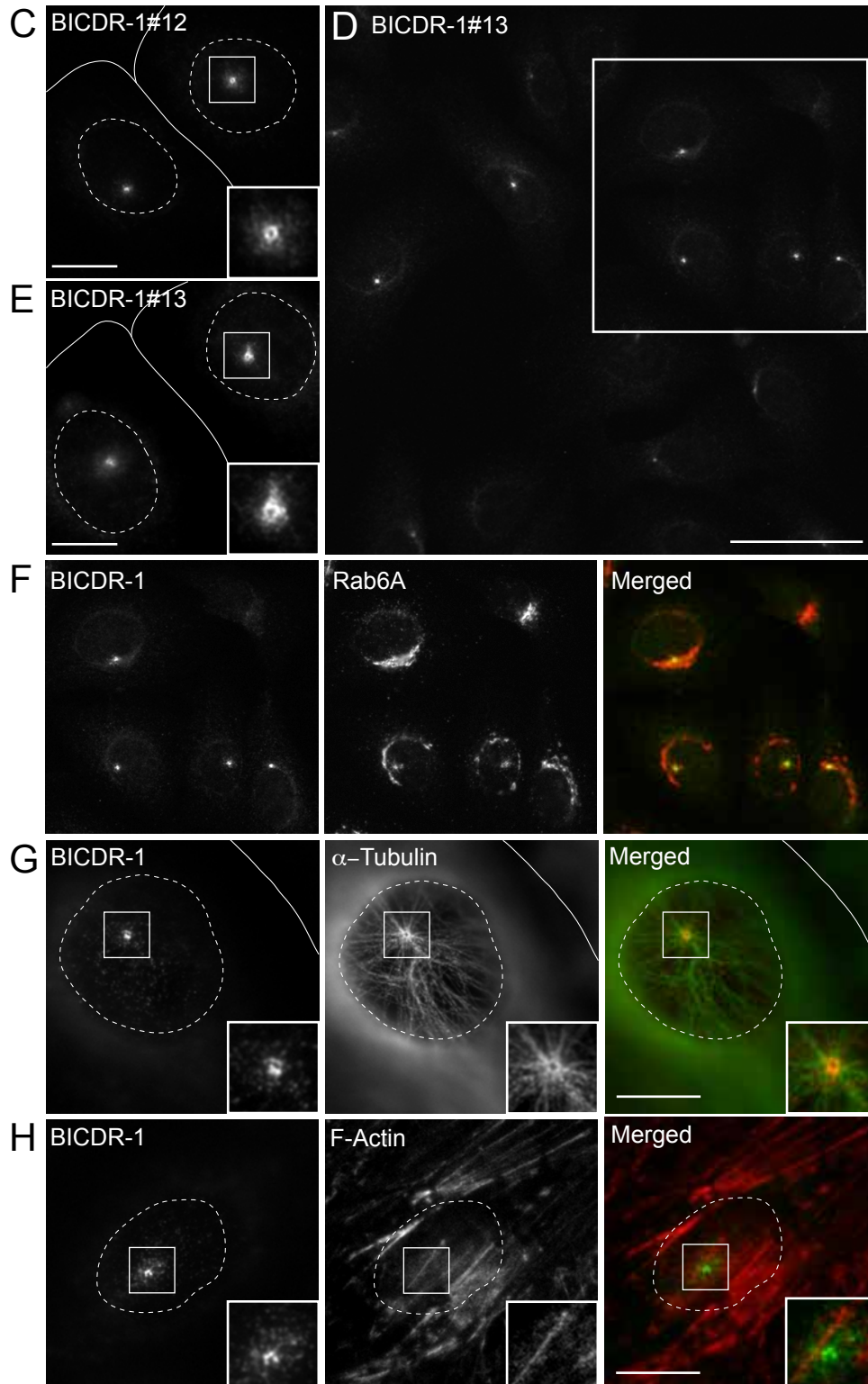
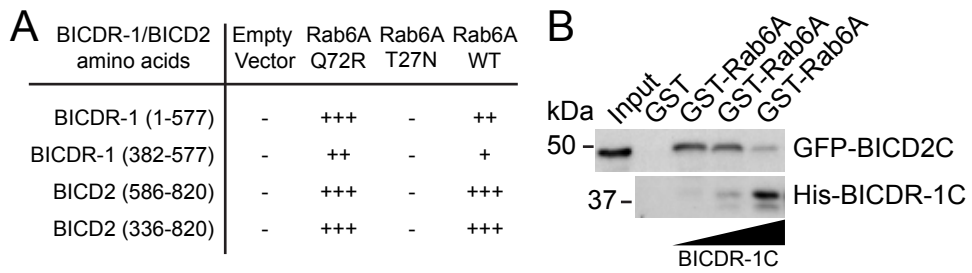
B



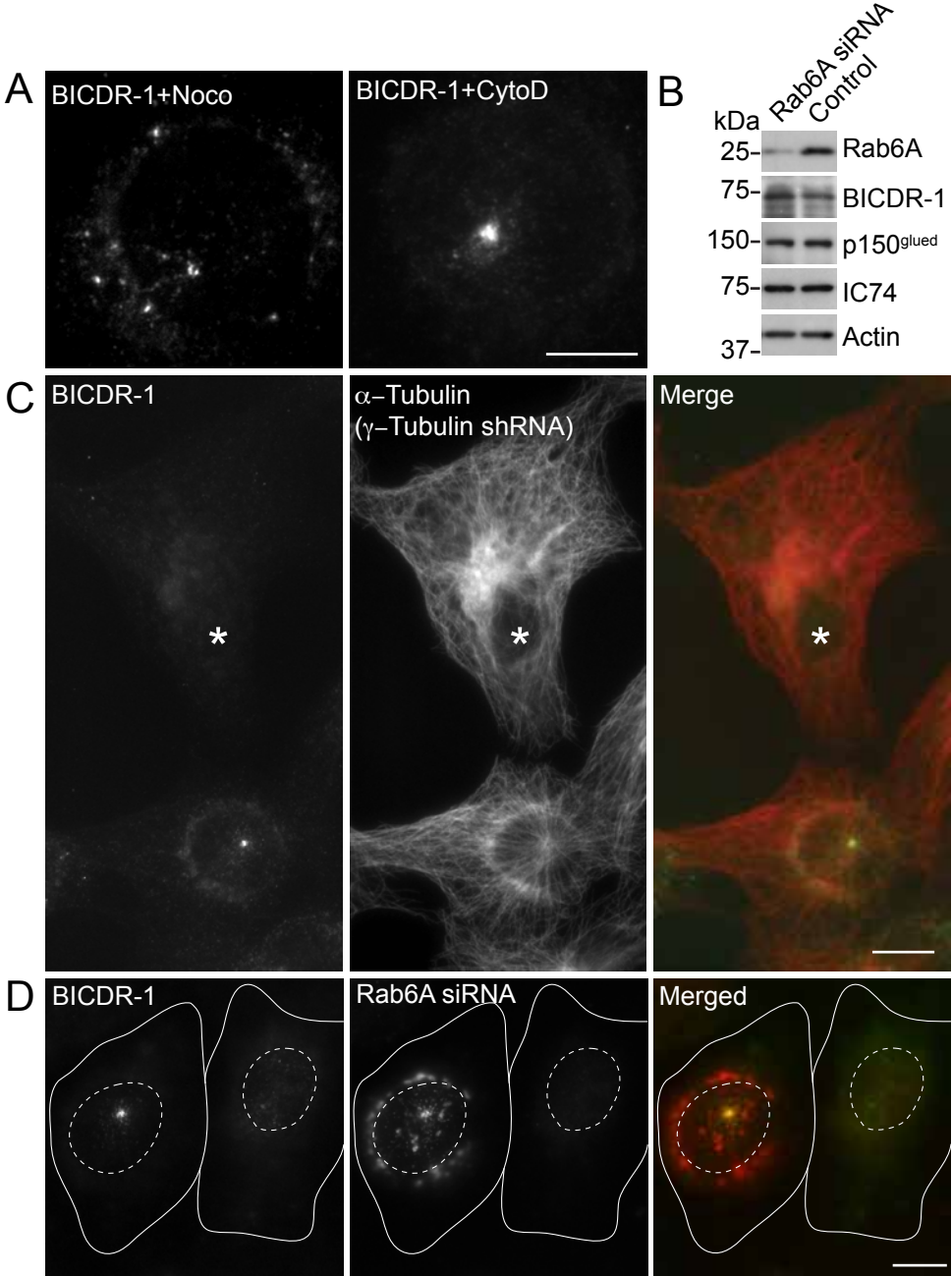
C

BICD1	1	MAAEE-----ALKTV-----DQYKT-----EIE
BICD2	1	MSAPS-----EEEEYARLVMEAQPEWTRA-----EIVK
BICDR-1	1	MSAFCLGLAGRASAPAEPPDSACCMELPAGAGDAVRSPATAAALVSFPGGPGELELALLEELALLAAGERSSEPGEHPQAEPEPVEGHGPPPLPPPPTQDP
BICDR-2	1	MDS-----PGEP-----SFPSGLLGGGASPS-----GDEGFFPVLERRDSFLGGG-----PGPEEPE
BICD1	19	RLTKELTETTHEKIQAAEYGLVVLLEEKLTLKQOYDELEAEYDGLKQELEQLREAFGQSFSIHRKVAEDGETREETLLOESASKEAYYLNKILEMQLNELKQ
BICD2	28	RLSHELAEATTREKIQAAEYGLAVLEEKHQKLLQFEELVDYEAIRSEMQLKEAFGQAHTNHKKVAADGSSREESLIQESASKEQYYVRKVLLELQTELKQ
BICDR-1	101	ELLSVIRQEKEDLVLAARLKGKALLERNQDMSRQYEQMHKELTDKLEHLEQ---EKHELRRRFENREGEWEGRVSELETDVKQLQDELERQQHLHREADRE
BICDR-2	49	DIALQLQQEKDLLLAELGKMLLERNEELRRQLETINTQHLHEERLQQ---ENHELRRGLAARGAEWBARAVELEGDVEALRAQLGEQRSERQDSGRE
BICD1	119	SRAVVTNVQAENERLISAVVQELKENNEMVELQIRIRMKDEIRYKFRARLLQDYTELLEENITLQKLVSTLKQNVQVEYEGLEKHEIKRFEETVLLNSQLE
BICD2	128	LRNVLTNTQSENERLTSVAQELKEINQNVIEIQGRRLRDDIKYKFRARLLQDYSELLEENISLQKQVSVLRQNVQVEFEGLEKHEIKRLEETEYVLLNSQLE
BICDR-1	198	KTRAVQELSEQNQLRLDQLSRASEVERQLSMQVHALKEDFREKNSSTNQHIRLESQAIEIKMLSDRKREI---EHLRSATLEENDLLQGT-----
BICDR-2	146	RARALGELSEQNQLRISQQLAQASRTEQELQRELDLTRERCQTALAGAEELGARLESQAENQMLQDRRQDI---EAQIRGLREVDKQGNR-----
BICD1	219	DAIRLKEIAEHQLEEALETLNKEREQKNNLRKELSQYINLSDS----HISISVDGLKFAEDG--SEPNNDDK--MNGHIHGPLGKLNQDYRTPTRKGES
BICD2	228	DAIRLKEISERQLEEALETLNKEREQKNNLRKELSHYMSINDSFYTSHLQVSLDGLKFSDDTVTAEPNNDAAEALVNGFEHSLGVLKSSLDNKTSTPRKDGL
BICDR-1	286	-----
BICDR-2	234	-----
BICD1	311	LDP----VSDLFSELNISEIQKQKQQLIQVEREKAILLANLQESQTOLEHTKGALTEQHERVHRLTEHVNAMRGLONSKEIKAELEDCCKGRNSAAEEAHDY
BICD2	328	APPSPSLVSDLLSELHISEIQKQKQQLVQMEREKVGLLATLQDTOKOLEQARGTLEQHEKVNRLTENLSALRRLQAGKERQTSIDNEKDRDSDHEDGDYY
BICDR-1	286	-----VEELQDRVLILERQGHDKDLOLHQSOLELQEVRLSYRQLQGVVEELTEERS---LOSSAATSTSLSEIEQSMEAELEEQ
BICDR-2	234	-----LQTTHEELLLLRRERKEKHELEERARFEAGEALRTLRLGLQRRVSELEEEER---LQDTEISGASLQTELAHSLDSDQDQD
BICD1	407	EVDINGLEILECKYRVAVTEVIDLKAELKALKEKYNKSVENYTEEKTKEYESKIOMYDEQVTNLEKTSKESGKMAHMEKELQKMTGIANENHNTLNTAQD
BICD2	428	EVDINGPEILACKYHVAVAEAGELREQLKALRSTHEAREAQAHEEKGRYEAEGQALTEKISLLEKASHQDRELLAHLEKELKVVSDVAGETQGSNLVAQD
BICDR-1	363	EREQLRLQLWEAYCQVRYLC-----SHLRGNDSDADSA
BICDR-2	311	QQ-----V-----NECGGSQAILSP
BICD1	507	ELVTFSEELAQLYHHVCLCNNETPNRVMLDYRQSRVTRSGSLKGPDDPRGLLSPRLSRRGVSSPVESRTSSEPVSSENTETSKEPSPTKTPTTISPVITA
BICD2	528	ELVTFSEELANLYHHVCMCNNETPNRVMLDYREG---QGKAGRTSPEGRGRRSPVLLPKGLLATEVGRADGGTGDNSPSPSSSLPSP-----
BICDR-1	395	VTDSSMDESSETSSAKDVPAGSLRT-----
BICDR-2	326	ETQETS SPQPSIQEEILEPPKKRASL-----
BICD1	607	PPSSPVLDTSDIRKEPMNIYNLNAIVRDIKHLQKAVDRSLQSRQRAAARELAPMIDKDKEALMEEILKLSLSTKREQIATLRAVLKANKQTAEVAL
BICD2	613	-----LSDPRREPMNIYNLAIIRDQIKHLQAAVDRTTLELSRQRIASQELGPAVDKDKEALMEEILKLSLSTKREQITLRLTVLKANKQTAEVAL
BICDR-1	421	---ALNDLKRLIQSIIVDGEPTVTLSSVEMTALKEERDRLRVTSSEDKPEKQLQKAIKIR-----
BICDR-2	352	---SPVEILEEKEAEVARLQDEITLHRTTELQTLRDELQROKELRAQDNPEEALSSALS-----
BICD1	707	ANLNKKNYENKAMVTETMTKLRNELKALKEDAATFSSLRAMFATRCDEYVTQLDEMQRQLAAAEDEKKTLENTLLRMAIQOKLALTORLELEDFDHE----
BICD2	705	ANLKSKEYENKAMVTETMTMMLRNLKALKEDAATFSSLRAMFATRCDEYITQLDEMQRQLAAAEDEKKTLENSLLRMAIQOKLALTORLELELEDFDHE----
BICDR-1	476	-----DR-DEAIAKKNAVELELAKCKMDMMSLSNQLLDAIQOKLNLSSQOLEAWQDDMHRVID
BICDR-2	407	-----DR-DEAVNKAMKLSLELSRVSLERDSLSRELLRAIRQKVALTORLELEAWQDDMQVIVIG
BICD1	803	-----QSRRSKSGKLGKSKIGSPKIVSSLPPYRHSAHN 835
BICD2	801	-----QTRRGRSKAASKAKPASPSSL----- 820
BICDR-1	532	RQLMDTHLKEQSRPAAAAFPGRGHGVG-RGQEPSTADGKRLFSFFRKI--- 577
BICDR-2	463	QQLRSQRQKELSE-AAAAPRRRAKTRF-SLRLGSGQSGGFLSNLFRRT--- 507

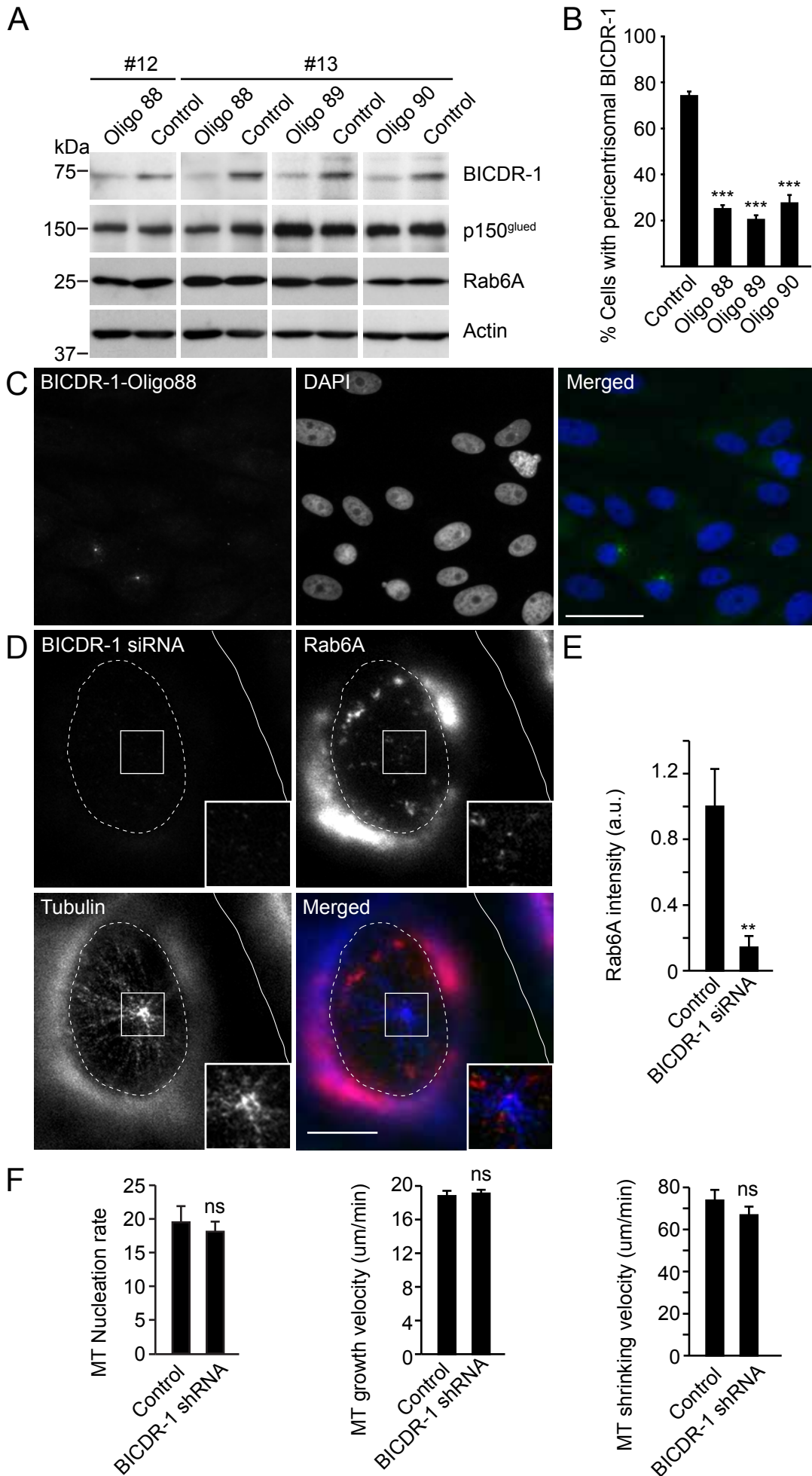
Schlager et al., Supplemental Figure 2



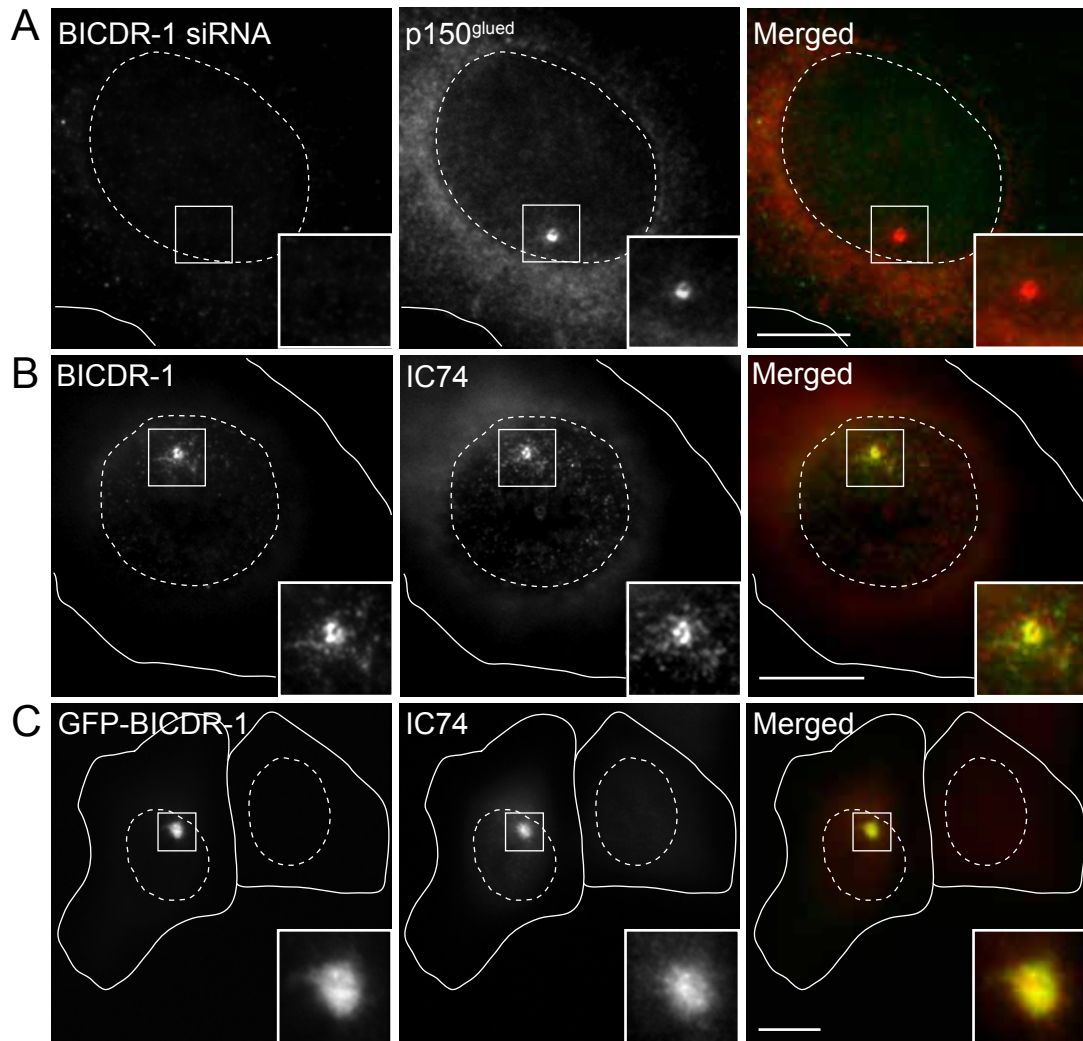
Schlager et al., Supplemental Figure 3



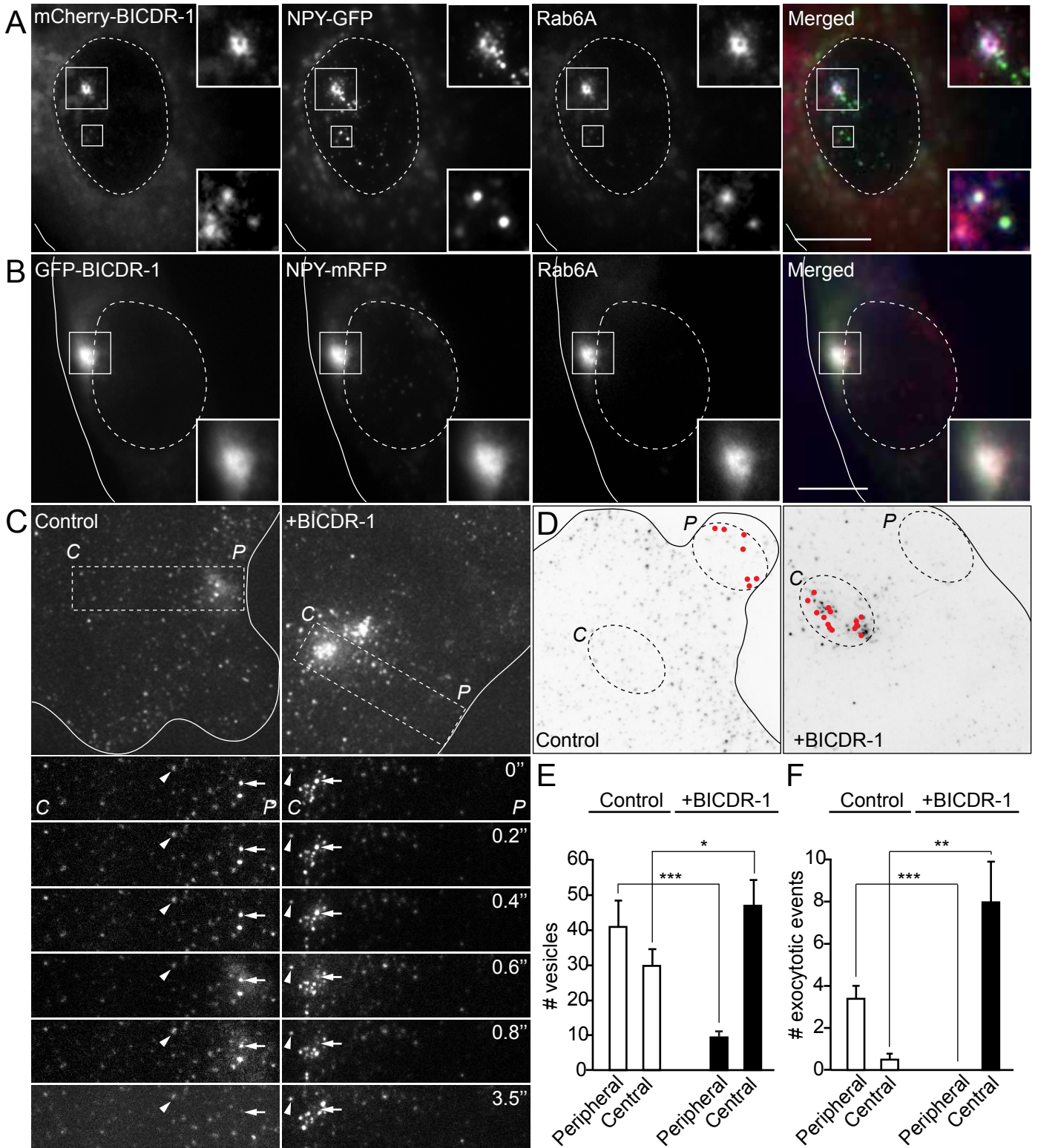
Schlager et al., Supplemental Figure 4



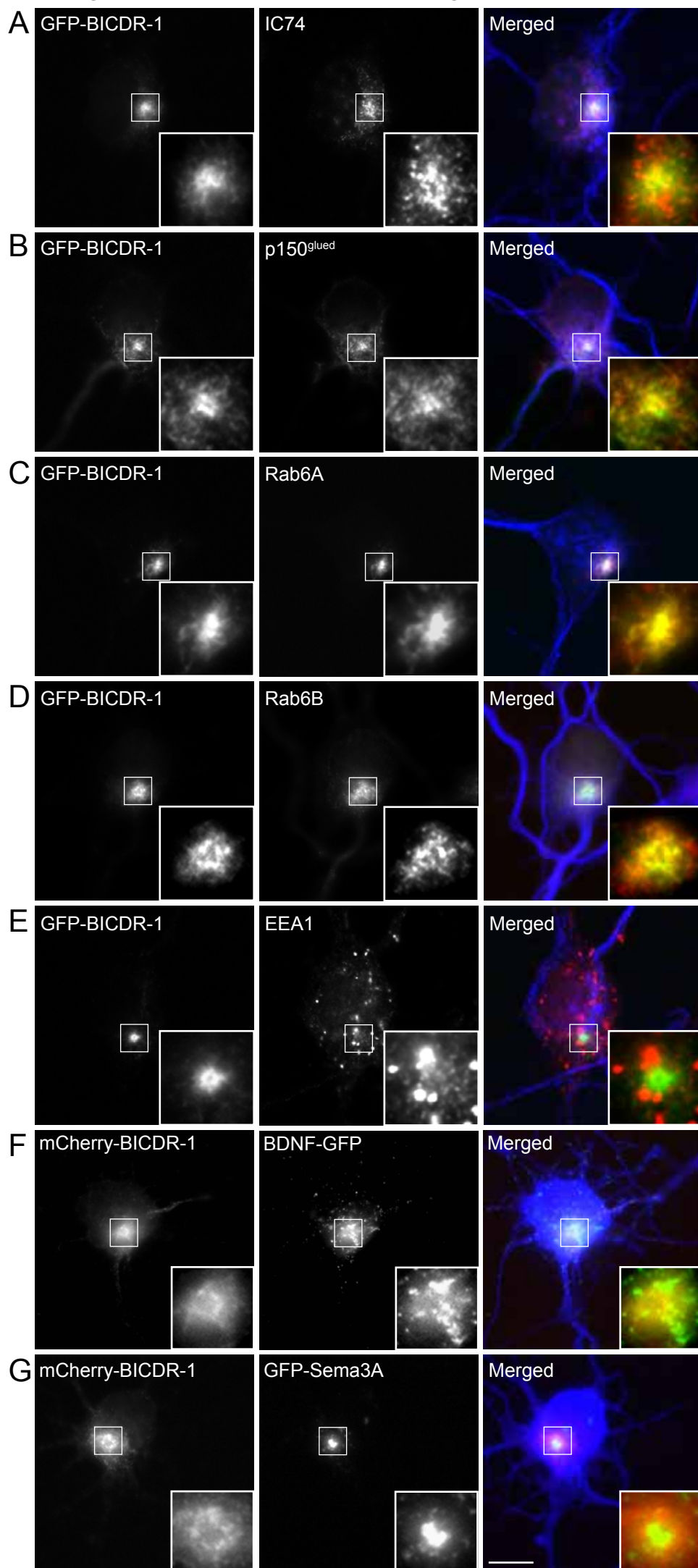
Schlager et al., Supplemental Figure 5



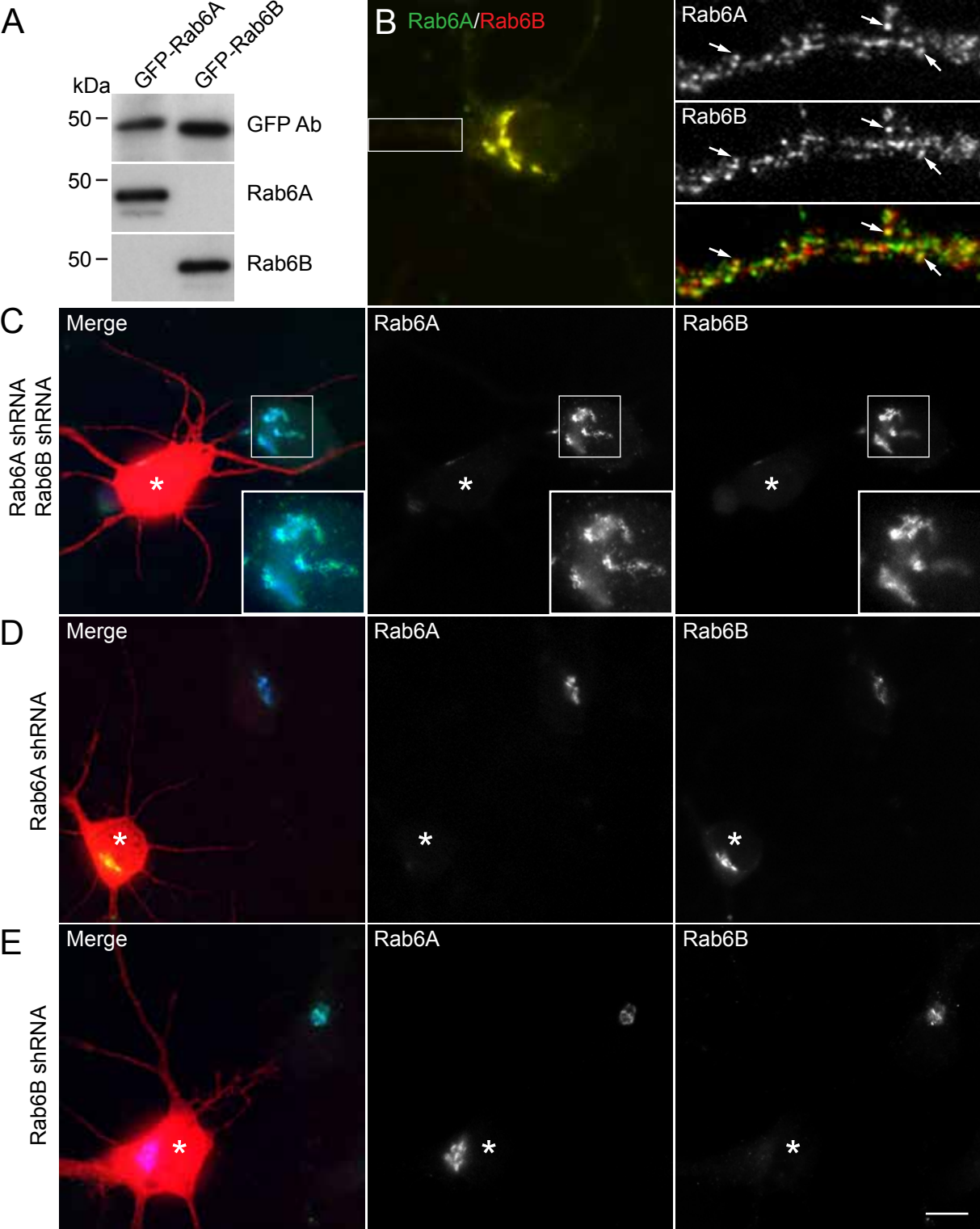
Schlager et al., Supplemental Figure 6



Schlager et al., Supplemental Figure 7



Schlager et al., Supplemental Figure 8



Schlager et al., Supplemental Figure 9

